

The structure and magnetic properties of a 3D pillared-layer polymer and two helical chains constructed from flexible ligands

Long Tang^a, Dongsheng Li^{a,*}, Feng Fu^a, Yapan Wu^a, Yaoyu Wang^{b,*},
Huaiming Hu^b, Enbo Wang^c

^a Department of Chemistry and Chemical Engineering, Shaanxi Key Laboratory of Chemical Reaction Engineering, Yan'an University, Yan'an, Shaanxi 716000, China

^b Department of Chemistry, Shaanxi Key Laboratory of Physico-Inorganic Chemistry, Northwest University, Xi'an, Shaanxi 710069, China

^c Institute of Polyoxometalate Chemistry, Department of Chemistry, Northeast Normal University, Changchun 130024, China

Received 7 November 2007; received in revised form 20 December 2007; accepted 21 December 2007

Available online 10 January 2008

Abstract

Three novel coordination polymers of Co^{II} and Cu^{II} with flexible ligands, namely [Co(oba)(dpa)]_n (**1**), [Cu(oba)(dpa)]_n (**2**) and [Cu(oba)(bpy)_{1/2}]_n (**3**) [H₂oba = 4,4'-oxybis(benzoic acid), dpa = 2,2'-dipyridylamine, bpy = 4,4'-bipyridine] were synthesized by hydrothermal reactions and characterized by single-crystal X-ray diffraction, thermogravimetric analyses, elemental analysis and IR spectroscopy. X-ray diffraction analysis reveals that complexes **1** and **2** are isostructural. In complexes **1** and **2**, the Co^{II} and Cu^{II} ions are linked by flexible oba ligands to form 1D helical chain. These chains are further assembled into 3D supramolecular edifice via aromatic π - π stacking interactions and intermolecular hydrogen bonding. The Cu^{II} ions in complex **3** are linked by the carboxylate groups oba to form an eight-membered ring chains, the connectivity between the corner-shared eight-membered ring chains are further bridged by the bent oba ligands to produce 2D helical layer containing the right-handed helical chains. Furthermore, the adjacent helical layers are connected by bpy pillars to form a novel 3D framework with an unprecedented topology of (3¹⁵·4²⁰·5⁸·6²). The magnetic properties of complexes **1–3** have also been investigated.

© 2008 Elsevier B.V. All rights reserved.

Keywords: Coordination polymer; Pillared-layer; Helical chains; Magnetic properties; Cobalt; Copper

1. Introduction

The current interest in the crystal engineering of coordination polymer frameworks not only stems from their potential applications in chemical separations, ion exchange, microelectronics, nonlinear optics, porous materials and catalysis, but also from their intriguing variety of architectures and topologies [1,2]. Therefore, a variety of coordination polymers with interesting compositions, architectures and topologies have been prepared through

taking certain factors into account, such as the coordination nature of the metal ion and the shape, functionality, flexibility and symmetry of organic ligand [3], of which many are derived from dicarboxylate ligands because of their interesting structural characteristics [4]. Thus, the prospect of tuning the properties of metal-organic frameworks through a systematic change of the organic ligands provides an impetus to further research of metal-organic supramolecular architectures. Lately, a series of open metal-organic frameworks with various structural motifs, including honeycomb, brick wall, bilayer, ladder, herringbone, diamondoid and rectangular grid, have been deliberately designed, and discussed in comprehensive reviews by Yaghi, Kitagawa, Rao and their co-workers [5]. Typically, the as-synthesized porous frameworks can be divided into

* Corresponding authors. Fax: +86 911 2332317 (D. Li); +86 29 88373398 (Y. Wang).

E-mail addresses: lidongsheng1@126.com (D. Li), wyaoyu@nwu.edu.cn (Y. Wang).

three groups, namely, metal–organic frameworks having multidimensional channels, pillared-layer architectures, and 3D nanotubular structures. Among them, pillared-layer architectures, which have been proven to be an effective and controllable route to design 3D frameworks with large channels [6–9]. Employing this approach, a variety of pillared-layer structures including positively and negatively charged or neutral layers have been synthesized [8]. This research area soon became very attractive because of the merits of pillared-layer structures, such as control over the porous structures and the chemical functionality by simple modification of the pillar module [10].

Helical structures have received much attention in coordination chemistry and materials chemistry, that mainly because helicity is an essence of life and is also important in advanced materials, such as optical devices, enantiomer separation, chiral synthesis, ligand exchange, biological systems and, selective catalysis [11–15]. Many chemists have made great contributions to this field, and the design of helical coordination polymers through the self-assembly of ligands and metal cations has shown significant progress recently [13,14]. However, the occurrence of pillared-layer complexes with helical character is particularly rare. Furthermore, multidentate N- or O-donor ligands have been extensively employed in the construction of pillared-layer structures. For example, as an excellent candidate for rigid rodlike organic building units, exo-bidentate 4,4'-bipyridine (bpy) has been relatively well-known and shows many interesting supramolecular architectures [16]. Dicarboxylate ligands can bridge two or more different metal centers and produce neutral architectures [17–19]. Hence, metal–organic coordination polymers constructed by mixed ligands of pyridyl groups and carboxylate groups, which not only incorporate interesting properties of different functional group [17], but also are more adjustable through changing one of the above two organic ligands [18,19]. For instance, using dipyridyl ligands as pillars between the neutral layers of dicarboxylate and metal ions, a few three-dimensional layer-pillar complexes have been constructed [19]. And yet, because of the difficult prediction of either the composition or the structure of the reaction product [20], the architectures of coordination polymers from mixed ligands and metal ions are still a long-term challenge to chemists, especially those from flexible bridging ligands because of their flexibility and conformational freedom in assembly process [21]. Consequently, a great deal of work is required to extend the knowledge of relevant structural types and establish proper synthetic strategies leading to desirable architectures and useful properties.

In our strategy, 4,4'-oxybis(benzoic acid) (H₂oba) is a typical example of long V-shaped ligands, it has proven to be able to establish bridges between metal centers. Its coordination chemistry has been studied and some coordination polymers have been obtained [22]. Because of its two oxo carboxylate groups, H₂oba can coordinate to metal ions in didentate, tridentate, tetradentate, pentadentate and hexadentate modes. To investigate the effects of

rigid and flexible exo-bidentate pyridyl-containing ligands on conformations of H₂oba as well as the assembly process of H₂oba and metal ions, the hydrothermal reactions of H₂oba with M(II) and multidentate N-donor ligands were carried out, and a series of coordination polymers were obtained. Herein, we report the syntheses and characterizations of three novel M(II) compounds exhibiting different topologies: [Co(oba)(dpa)]_n (**1**), [Cu(oba)(dpa)]_n (**2**) and [Cu(oba)(bpy)_{1/2}]_n (**3**). The magnetic properties of complexes **1–3** have also been investigated.

2. Experimental

2.1. Materials and chemical analysis

The H₂oba, bpy and dpa ligands were purchased in the Alfa Aesar company; all other reagents and solvents employed were commercially available and used without further purification. The C, H and N microanalyses were carried out with a Vario EL elemental analyzer. The IR spectra were recorded with a Nicolet Avatar 360 FT-IR spectrometer using the KBr pellet technique. Thermogravimetric curves were measured on a Perkin-Elmer TGA-7 (USA) at a heating rate of 10 °C min⁻¹ from room temperature to 700 °C under nitrogen. The powder X-ray diffraction patterns were recorded on a Shimadzu XRD-7000 diffractometer. The magnetic susceptibilities were obtained on crystalline samples using a Quantum Design MPMS SQUID magnetometer. The experimental susceptibilities were corrected for the sample holder and the diamagnetism contributions estimated from Pascal's constants.

2.2. Synthesis of [Co(oba)(dpa)]_n (**1**)

A mixture of Co(NO₃)₆·6H₂O (0.1 mmol), H₂oba (0.1 mmol), dpa (0.1 mmol) and triethylamine (1.2 mmol) and water (10 ml) was stirred for 20 min in air. The mixture was then transferred to a 23 ml Teflon reactor and kept at 140 °C for 5 days under autogenous pressure, and then cooled to room temperature at a rate of 5 °C h⁻¹. Red crystals of **1** were obtained (yield: 69% based on Co). Elemental analysis. Calcd for C₂₄H₁₇N₃O₅Co: C, 59.27; H, 3.52; N, 8.64%. Found: C, 59.45; H, 3.16; N, 8.77%. IR data (KBr cm⁻¹): 3320(m), 1649(vs), 1458(s), 1510(s), 1486(s), 1402(w), 1335(s), 1254(w), 1148(m), 1079(m), 1017(w), 870(m), 769(m), 721(w), 678(m).

2.3. Synthesis of [Cu(oba)(dpa)]_n (**2**)

Complex **2** was prepared as for **1** by using Cu(NO₃)₃·3H₂O instead of Co(NO₃)₆·6H₂O. Blue crystals of **2** were obtained (yield: 64% based on Cu). Elemental analysis. Calcd for C₂₄H₁₇N₃O₅Cu: C, 58.71; H, 3.49; N, 8.56%. Found: C, 59.15; H, 3.27; N, 8.76%. IR data (KBr cm⁻¹): 3323(m), 1641(vs), 1462(s), 1514(s), 1482(s), 1406(w), 1335(s), 1252(w), 1153(m), 1087(m), 1018(w), 870(m), 775(m), 721(w), 687(m).

2.4. Synthesis of $[Cu(oba)(bpy)]_{12} (3)$

A mixture of $Cu(NO_3)_2 \cdot 3H_2O$ (0.1 mmol), H_2oba (0.1 mmol), bpy (0.1 mmol), and water (10 mL) was placed in a Teflon reactor (23 mL). The pH was adjusted to 7.0 by addition of triethylamine, the mixture was heated at 160 °C for three days, and then it was cooled to room temperature at 5 °C h⁻¹. Blue crystals of **3** were obtained in 52% yield based on Cu. Elemental analysis (%). Calcd for $C_{19}H_{12}CuNO_5$: C 57.36, H 3.04, N 3.52. Found: C 57.95; H 3.21; N 4.01; IR data IR (KBr cm⁻¹) (KBr cm⁻¹): 3436(w), 3063(w), 2924(w), 1594(vs), 1551(m), 1499(m), 1393(s), 1299(w), 1240(s), 1221(m), 1159(m), 1013(w), 877(m), 779(m), 675(w), 565(w), 514(w).

2.5. X-ray crystallographic studies

Diffraction intensities for the three complexes were collected at 293 K on a Bruker SMART 1000 CCD diffractometer employing graphite-monochromated Mo-K α radiation ($\lambda = 0.71073 \text{ \AA}$). A semi-empirical absorption correction was applied using the SADABS program [23]. The structures were solved by direct methods and refined by full-matrix least-squares on F^2 using the SHELXS 97 and SHELXL 97 programs, respectively [24,25]. Non-hydrogen atoms were refined anisotropically and hydrogen atoms were placed in geometrically calculated positions. The crystallographic data for complexes **1–3** are listed in Table 1, and selected bond lengths and angles are listed in Table 2.

3. Results and discussion

3.1. Description of the structures

The oba ligands in complexes **1–3** are completely deprotonated and are significantly bent at the ether–oxygen sites [$C-O-C = 116.6(7)–119.1(3)^\circ$]. They afford several kinds of coordination modes: bis(chelating bidentate) and bis(bridging-bidentate) (see Scheme 1).

3.1.1. Structure of $[Co(oba)(dpa)]_n (1)$ and $[Cu(oba)(dpa)]_n (2)$

X-ray diffraction analysis reveals that compounds **1** and **2** are isostructural, and the structure of **1** will be discussed in detail as a representative example, the structure of **2** can be found in the Supporting Information (Figs. S1–S3). The asymmetric unit of **1** consists of one crystallographic independent Co(II) atom, one oba ligand and one dpa ligand. The Co(II) ion is located in a slightly distorted octahedral geometry and is coordinated to four oxygen atoms of two oba ligands and two nitrogen atoms of one dpa ligand, as shown in Fig. 1. The average Co–N bond length is 2.056(4) Å and the Co–O bond lengths are in the range 2.112(3)–2.182(3) Å. The details are depicted in Table 2. Each oba ligand adopts a bis(chelating bidentate) mode (see Scheme 1 (I)), linking two Co(II) ions.

The adjacent Co(II) ions are bridged by V-shaped oba ligands to form a helical chain running along a -axis (Fig. 2). The helix is generated around the crystallographic 2_1 axis with a pitch of 12.125(2) Å. Notably, the two benzene rings of oba ligand are severely bent (the dihedral

Table 1
Crystal data and structure refinements for complexes **1–3**

Complex	1	2	3
Formula	$C_{24}H_{17}CoN_3O_5$	$C_{24}H_{17}CuN_3O_5$	$C_{19}H_{12}CuNO_5$
M_r [g]	486.34	490.95	397.84
Crystal system	Monoclinic	Monoclinic	Monoclinic
Space group	$P2(1)/c$	$P2(1)/c$	$C2/c$
a [Å]	12.125(2)	12.391(2)	22.1792(17)
b [Å]	15.700(3)	15.590(3)	13.6526(11)
c [Å]	11.271(2)	11.297(2)	13.0343(10)
α [°]	90	90	90
β [°]	95.534(2)	96.219(3)	119.2810(10)
γ [°]	90	90	90
V [Å ³]	2135.6(5)	2169.6(7)	3442.6(5)
Z	4	4	8
ρ_{calcd} [g cm ⁻³]	1.513	1.503	1.535
μ [mm ⁻¹]	0.846	1.049	1.299
Collected reflections	9632	10742	8575
Unique reflections (R_{int})	3773(0.0597)	3822(0.1866)	3069(0.0385)
Observed reflections [$I > 2\sigma(I)$]	2089	1160	2277
Refined parameters	298	298	236
Goodness of fit	1.006	0.810	1.042
R_1^a/wR_2^b [$I > 2\sigma(I)$]	0.0496/0.0926	0.0639/0.0747	0.0381/0.0792
R_1^a/wR_2^b (all data)	0.1096/0.1196	0.0583/0.0898	0.0583/0.0898
Largest residuals [eÅ ⁻³]	0.308/–0.535	0.412/–0.457	0.323/–0.335

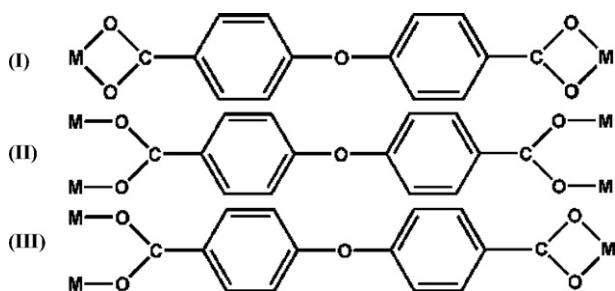
^a $R_1 = \sum ||F_o| - |F_c|| / \sum |F_o|$.

^b $wR_2 = [\sum w(F_o^2 - F_c^2)^2 / \sum w(F_o^2)^2]^{1/2}$.

Table 2
Selected bond lengths (Å) and angles (°) for complexes 1–3^a

Complex 1		Complex 2		Complex 3	
Co(1)–N(2)	2.051(4)	Cu(1)–N(1)	1.989(6)	Cu(1)–O(1)	1.952(2)
Co(1)–N(1)	2.061(4)	Cu(1)–O(1)	2.435(5)	Cu(1)–O(4B)	1.985(2)
Co(1)–O(1)	2.112(3)	Cu(1)–O(3)	2.452(5)	Cu(1)–O(2C)	2.172(2)
Co(1)–O(4)	2.168(3)	Cu(1)–N(2)	1.970(6)	O(4)–Cu(1D)	1.985(2)
Co(1)–O(2)	2.181(3)	Cu(1)–O(2)	2.016(5)	Cu(1)–O(5A)	1.968(2)
Co(1)–O(3)	2.182(3)	Cu(1)–O(4)	2.014(5)	Cu(1)–N(1)	1.999(2)
N(2)–Co(1)–N(1)	91.10(14)	N(2)–Cu(1)–N(1)	93.2(3)	O(2)–Cu(1C)	2.172(2)
N(2)–Co(1)–O(1)	102.70(13)	N(1)–Cu(1)–O(4)	90.8(2)	O(5)–Cu(1E)	1.968(2)
N(1)–Co(1)–O(1)	105.74(13)	N(1)–Cu(1)–O(2)	158.7(3)	O(1)–Cu(1)–O(5A)	99.58(9)
N(2)–Co(1)–O(4)	94.49(13)	N(2)–Cu(1)–O(1)	102.8(2)	O(5A)–Cu(1)–O(4B)	85.86(9)
N(1)–Co(1)–O(4)	95.39(12)	O(4)–Cu(1)–O(1)	102.5(2)	O(5A)–Cu(1)–N(1)	172.03(10)
O(1)–Co(1)–O(4)	152.27(12)	N(2)–Cu(1)–O(3)	94.7(2)	O(1)–Cu(1)–O(2C)	100.50(9)
N(2)–Co(1)–O(2)	163.88(13)	O(4)–Cu(1)–O(3)	58.55(18)	O(4B)–Cu(1)–O(2C)	103.60(9)
N(1)–Co(1)–O(2)	94.11(14)	O(1)–Cu(1)–O(3)	156.3(2)	O(1)–Cu(1)–O(4B)	155.34(10)
O(1)–Co(1)–O(2)	61.19(12)	N(2)–Cu(1)–O(4)	153.2(2)	O(1)–Cu(1)–N(1)	87.86(10)
O(4)–Co(1)–O(2)	100.18(12)	N(2)–Cu(1)–O(2)	94.6(3)	O(4B)–Cu(1)–N(1)	88.54(10)
N(2)–Co(1)–O(3)	92.61(13)	O(4)–Cu(1)–O(2)	91.1(2)	O(5A)–Cu(1)–O(2C)	89.51(9)
N(1)–Co(1)–O(3)	155.95(13)	N(1)–Cu(1)–O(1)	100.6(2)	N(1)–Cu(1)–O(2C)	86.31(9)
O(1)–Co(1)–O(3)	96.60(12)	O(2)–Cu(1)–O(1)	58.33(18)	O(1)–Cu(1)–Cu(1D)	76.69(7)
O(4)–Co(1)–O(3)	60.63(11)	N(1)–Cu(1)–O(3)	94.1(2)	O(5A)–Cu(1)–Cu(1D)	75.38(7)
O(2)–Co(1)–O(3)	88.82(12)	O(2)–Cu(1)–O(3)	104.9(2)	N(1)–Cu(1)–Cu(1D)	109.39(7)
C(5)–O(5)–C(12A)	117.3(4)	C(12A)–O(5)–C(5)	116.6(7)	C(8)–O(3)–C(5)	119.1(3)

^a Symmetry operations: for 1: (A) $x-1, -y+1/2, z-1/2$; for 2: (A) $x+1, -y+1/2, z+1/2$; for 3: (A) $x, y+1, z$; (B) $-x+1, y+1, -z+3/2$; (C) $-x+1, -y+1, -z+2$; (D) $-x+1, y-1, -z+3/2$; (E) $x, y-1, z$.



Scheme 1. The coordination modes of oba²⁻ anions.

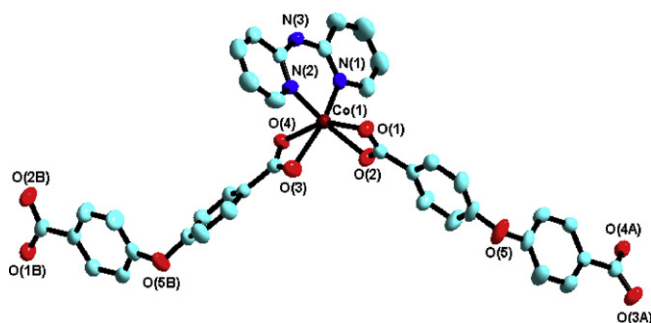


Fig. 1. The coordination environments of metal atoms in complex 1 with 30% thermal ellipsoids. All hydrogen atoms are omitted for clarity.

angle of the two benzene rings is ca. 80.9°). Obviously, this twist is an important factor in forming the helical structure. All dpa groups bristle out from the two sides of the helix, and the oba phenyl rings at each side of the helix are arranged in a parallel fashion with an interring distance of 25.737 Å. This orientation plays a critical role in packing

into a higher network through π – π stacking interactions between the dpa pairs.

Interestingly, through strong aromatic π – π stacking interactions between the dpa ligands (face-to-face 3.685 Å) and N–H···O hydrogen bonds between the dpa nitrogen atom (N(3)) and carboxyl oxygen atoms (O(4)) (N(3)···O(4) 2.886 Å and N(1)–H···O(2) 165.34°), the adjacent helical chains generate a 2D wavelike network with unusual parallelogram grids, and presents a (4,4) net in topology, as shown in Fig. 3. As a result, the cavity shape deviates from a regular square to a rhombus with size of about 21.377 × 15.729 Å along the two diagonal directions. The bent structure of oba contributes about 10 Å of the thickness of the layer, in which ether–oxygen sites of oba remarkably stick out from the plane. The network motif is similar to [Cu(oba)(2,2'-bpy)]_n [26], despite the large cavities, these layers stack along the *c*-axis without interpenetration. The thickness of the layer could inhibit the possibility of interpenetration. Otherwise the available void space of the grid is vacancy and the backbone is stabilized by N–H···O_{carboxylate} hydrogen bonds. Furthermore, those grids are enlarged to form the final 3D framework when viewed along the crystallographic *c*-axis (Fig. 4).

3.1.2. Structure of [Cu(oba)(bpy)_{1/2}]_n (3)

The coordination environment of the Cu(II) ions in complex 3 is shown in Fig. 5. The asymmetric unit of 3 consists of 26 non-hydrogen atoms, of which one Cu atom is crystallographically independent. The Cu(II) ions have a trigonal bipyramid geometry formed by four carboxylate

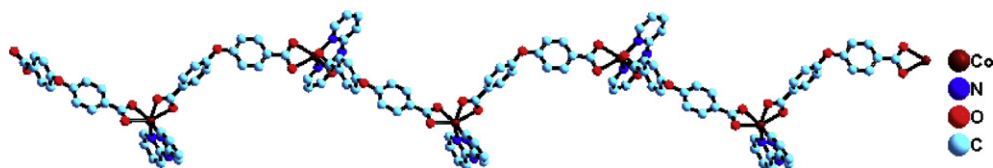


Fig. 2. The helical chain of complex 1 along the *a*-axis.

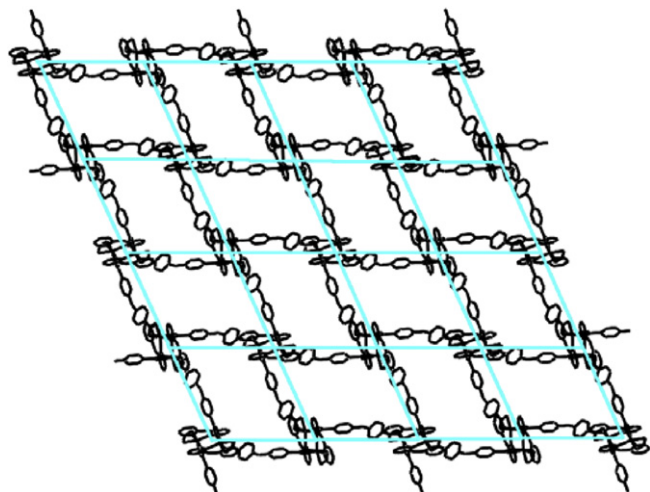


Fig. 3. View of 2D grid layer along the *ab* plane and the (4,4) net in complex 1.

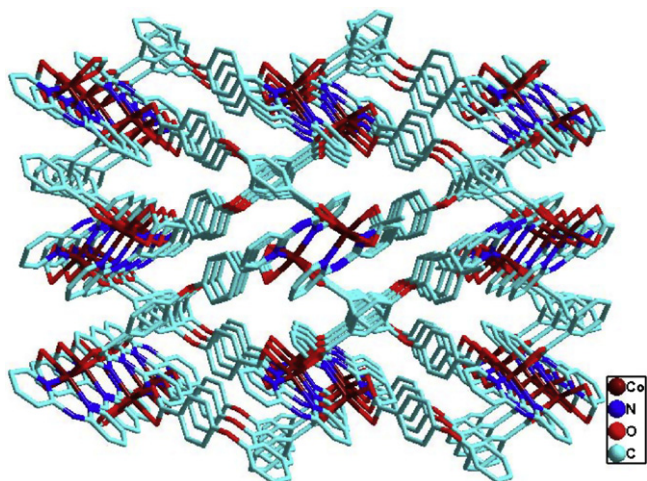


Fig. 4. The 3D supramolecular framework of complexes 1 viewed along the *c*-axis.

oxygen atoms and a nitrogen atom of the bpy. The Cu–O bond lengths are in the range 1.952(2)–2.172(2) Å, and the Cu–N bond distance has a value of 1.999(2) Å. So, the coordination geometry around the copper(II) atom can be regarded as a Jahn–Teller-distorted [27] trigonal bipyramid. The O/N–Cu–O/N bond angles are in the range 85.86(9)–172.03(10)°. There is only one oba anion present in the structure, and each oba ligand adopts a bis(bridging-bidentate) mode (see Scheme 1 (II)) and links four Cu(II) ions. The carboxylate groups of oba ligands have

connectivity with the Cu(II) cations forming an eight-membered ring chains, as shown in Fig. 6; in which the adjacent Cu···Cu distances are alternately 3.0195 Å and 4.414 Å. The bond distances and angles associated with the oba anions are in the ranges expected for this type of bonding [26,28]. The corresponding bond distances 3 are listed in Table 2.

The connectivity between the corner-shared eight-membered ring chains are further bridged by the bent oba ligands to produce 2D helical layers lying the *ac* plane (Fig. 7). When viewed along the *c*-axis, these 2D layers can be regarded as sine- and cosine-type curves intersecting at the zero points (see Fig. S4 in the Supporting Information). Of particular interest is that adjacent helical layers are connected by bpy as molecular pillars to form a novel 3D framework featuring with channels along *b*-axis (Fig. 8a). But the channels are too small to residue any guests. From a topological perspective, the structure of 3 reveals that it is a complicated 3D framework containing multiform adamantanoid cages. Considering the Cu atoms and the C atoms of the μ -carboxylate groups as nodes, we can see that the neutral (3,5)-connected layer of composition [Cu(oba)], these 2D sheets are further connected together in the third dimension by axially coordinating bpy ligands to give a unique (3,5)-connected 3D net with an unprecedented topology of (3¹⁵.4²⁰.5⁸.6²) (Fig. 8b). The potential free volume determined by PLATON [29] calculation is 281 Å³ per unit cell volume (3443 Å³) which represents 8.1% of void per unit volume for 3 (taking into account the van der Waals volume of the atoms).

The most fascinating structural feature of 3 is that the two distinct helical chains running along the different crystallographic axis coexist in the 3D network. One type of helices are right-handed helical chains, and built from bpy bridges between the Cu centers with a pitch of 13.034 Å running along the *c*-axis (Fig. S5(a and b) in the Supporting Information). These right-handed helical chains, the one-end coordinated bpy groups, are further grafted on the 3D network with helical channels (All oba²⁻ anions are omitted for clarity), as shown in Fig. 9a. The other type of helices are the double-stranded helices chains in the 2D helical layer and formed by the V-shaped oba ligands bridging Cu atoms, which is generated around the crystallographic 2₁ axis in the *b* direction with a pitch of 13.653 Å (Fig. 9b), displaying a same helical orientation to the former helix. A striking feature of 3 is the alternating interweaving of two types of helices along the *b*- and *c*-axis to construct a 3D framework (Fig. 9c). Herein, the bpy

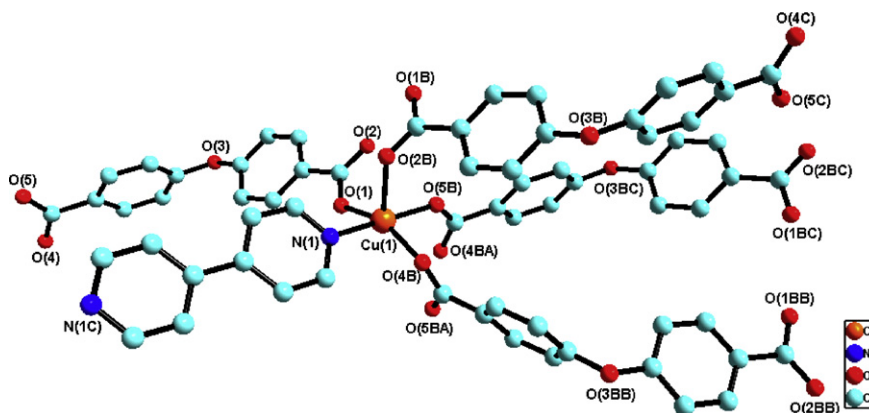


Fig. 5. The coordination environments of Cu atoms in complex 3. All hydrogen atoms are omitted for clarity.

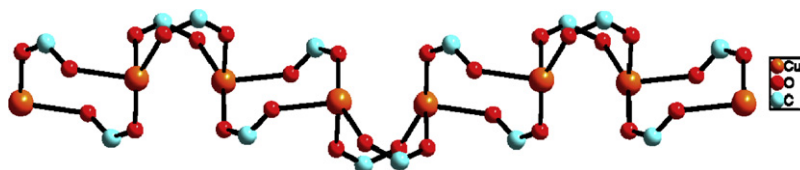


Fig. 6. The eight-membered ring chains of complex 3.

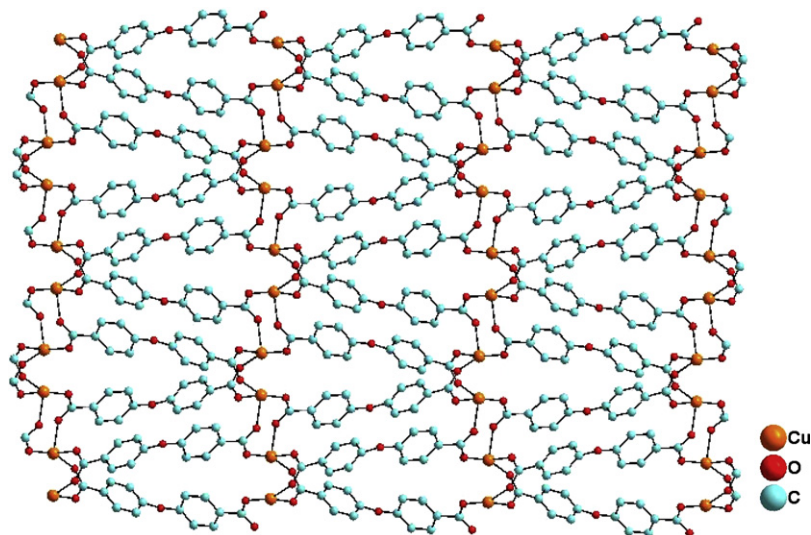


Fig. 7. The 2D helical layers of complex 3 viewed lying the *ac* plane.

molecules have both in-plane and out of plane connectivity. Viewing down the *c*-axis, the linkages between the Cu(II) ions and the oba anions are cross-linked by the bpy molecules.

3.2. Thermogravimetric analysis

To study the thermal stability of 1–3, thermogravimetric (TG) analyses were performed on polycrystalline samples under a nitrogen atmosphere (Figs. S6 and S7 in the Supporting information). TG curve of complex 1 illustrates that no weight losses were observed for either of the two

ligands up to 210 °C; after this, significant weight losses occurred and ended at ca. 525 °C, indicating the complete decomposition of the complex to form CoO, which was confirmed by X-ray powder diffraction analysis. This conclusion has been also supported by the percentage of the residues (15.67%), which is in accordance with the expected value (15.41%). The TG traces of 2 and 1 are analogous. Compared with 1 and 2, complex 3 exhibits relatively thermal stability. TGA analyses show that it has an onset temperature for decomposition above 300 °C. The stability of the complex makes it potential candidates for practical applications.

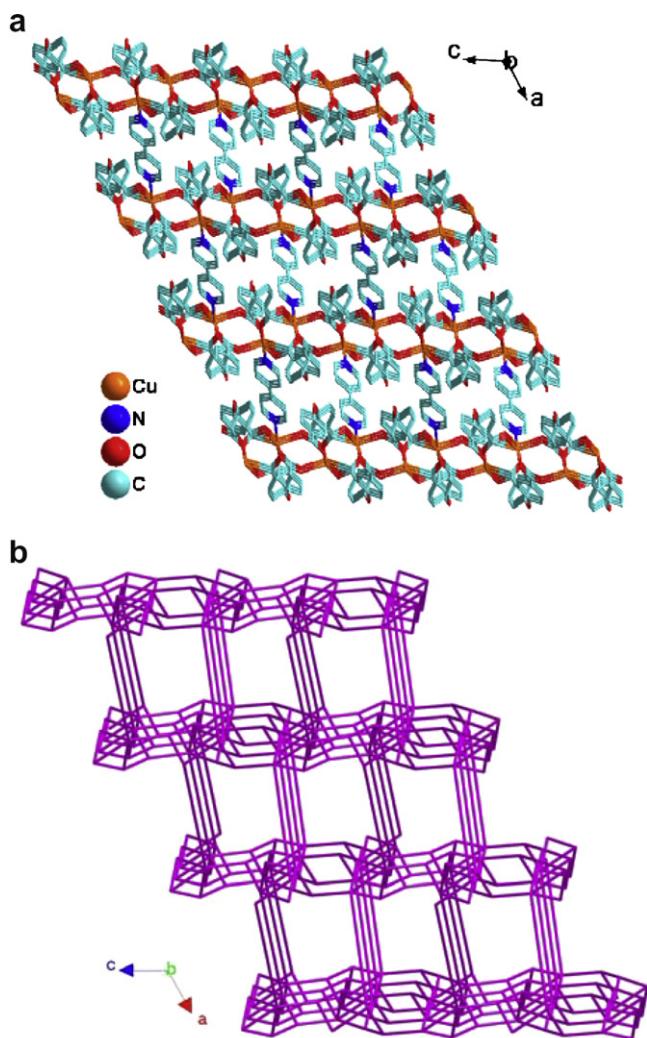


Fig. 8. (a) The 3D pillared-layer structure of complex **3** viewed along the *b*-axis; (b) schematic views of the (3,5)-connected net of $(3^{15}.4^{20}.5^8.6^2)$ topology of **3**.

3.3. Magnetic properties

Complexes **1** and **2** are isostructural, and the magnetic properties of complexes **1–3** were investigated over the tem-

perature range 5–300 K in here. The magnetic susceptibilities χ_M and $\chi_M T$ versus T plots are shown in Fig. 10. For complex **1**, the experimental $\chi_M T$ value at 300 K is $1.95 \text{ cm}^3 \text{ K mol}^{-1}$, somewhat larger than the spin-only value ($1.88 \text{ cm}^3 \text{ K mol}^{-1}$) expected for two isolated spin-only Co(II) ion ($S = 3/2$, Fig. 10a). The $\chi_M T$ value of **1** remains almost constant from 300 to 110 K, and then decreases on further cooling, reaching a value of $1.48 \text{ cm}^3 \text{ K mol}^{-1}$ at 5 K. This behavior indicates a weak antiferromagnetic interaction between the Co(II) ions in the structures. In **1**, the Co···Co distance through the oba bridge is 14.379 \AA . The temperature dependence of the reciprocal susceptibilities ($1/\chi_M$) obeys the Curie–Weiss law above 5 K with $\theta = -1.68 \text{ K}$, $C = 1.96$ and $R = 1.082 \times 10^{-4}$ ($R = \sum[(\chi_M)_{\text{obs}} - (\chi_M)_{\text{calc}}]^2 / \sum[(\chi_M)_{\text{obs}}]^2$). The values of θ for the complex **1** indicate weak antiferromagnetic interactions between the adjacent Co(II) ($S = 3/2$) ions.

For complex **2**, the experimental $\chi_M T$ value at 300 K is $0.87 \text{ cm}^3 \text{ K mol}^{-1}$, somewhat larger than the spin-only value ($0.75 \text{ cm}^3 \text{ K mol}^{-1}$) expected for two isolated spin-only Cu(II) ion ($S = 1$, Fig. 10b). As the temperature is lowered, the $\chi_M T$ value increases gradually, which indicating the presence of antiferromagnetic interactions in **2**. The temperature dependence of the reciprocal susceptibilities ($1/\chi_M$) obeys the Curie–Weiss law above 5 K with $\theta = -2.06 \text{ K}$, $C = 0.89$ and $R = 3.148 \times 10^{-4}$. The values of θ for the complex **2** indicate weak antiferromagnetic interactions between the adjacent Cu(II) ions.

For complex **3**, the $\chi_M T$ value at 300 K is $0.229 \text{ cm}^3 \text{ K mol}^{-1}$, which is much less than the expected value ($0.375 \text{ cm}^3 \text{ K mol}^{-1}$) of two isolated spin-only Cu(II) ions ($S = 1/2$, Fig. 10c). As T is lowered, $\chi_M T$ decreases continuously to a value of $0.045 \text{ cm}^3 \text{ K mol}^{-1}$ at 5 K. This behavior indicates a dominant antiferromagnetic interaction between the Cu(II) ions in the structures. As the shortest Cu···Cu distance across the carboxylate groups of oba ligands are alternately 3.0195 and 4.414 \AA in **3**, the magnetic exchange coupling through the oba ligands are expected to be very strong [30]. The observed antiferromagnetic interaction, therefore, should mainly arise from the magnetic superexchange through the $-\text{CO}_2$ bridge. The

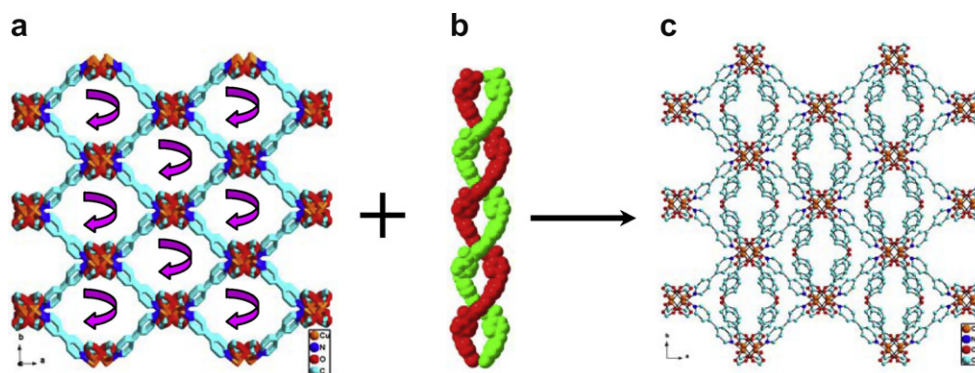


Fig. 9. (a) The 3D network with helical channels by bpy bridges in complex **3** viewed along the *c*-axis, all oba^{2-} anions are omitted for clarity. (b) Spacefilling diagram of the helical chains in the 2D helical layer. (c) The 3D network of complex **3** viewed along the *c*-axis.

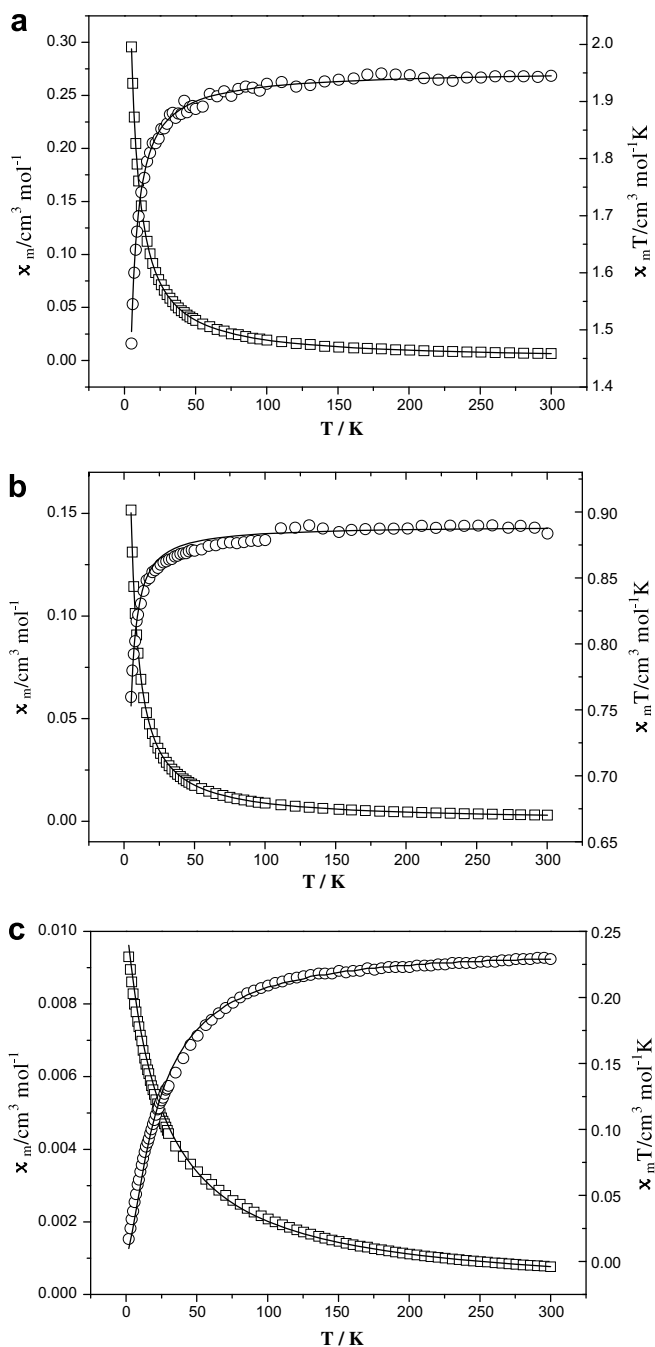


Fig. 10. a) Thermal variation of χ_M and $\chi_M T$ for compound **1**. (b) Thermal variation of χ_M and $\chi_M T$ for compound **2**. (c) Thermal variation of χ_M and $\chi_M T$ for compound **3**.

temperature dependence of the reciprocal susceptibilities ($1/\chi_M$) obeys the Curie–Weiss law above 5 K with $\theta = -23.9$ K, $C = 0.25$ and $R = 1.774 \times 10^{-4}$. The values of θ for the complex **3** exhibit very strong antiferromagnetic interactions between the adjacent Cu(II) ($S = 1/2$) ions.

To simulate the experimental magnetic behavior, we use the analytical expression for a one-dimensional Heisenberg chain of classical spins [$S = 1$] that similar to **1–3** [31].

$$\chi_M = \frac{Ng^2\beta^2 S(S+1)}{3KT} \frac{1+u}{1-u} \quad (1)$$

where

$$u = \coth \left[\frac{JS(S+1)}{kT} \right] - \left[\frac{kT}{JS(S+1)} \right]$$

Finally, this expression fits very well with the experimental susceptibilities of **1–3**, giving $J = -1.37$ cm⁻¹, $g = 2.04$, $R = 8.30 \times 10^{-5}$ for **1**, $J = -1.90$ cm⁻¹, $g = 2.18$ and $R = 3.406 \times 10^{-5}$ for **2** and $J = -23.0$ cm⁻¹, $g = 1.90$ and $R = 1.018 \times 10^{-3}$ for **3**, the agreement factor defined as $R = \sum[(\chi_M)_{\text{obs}} - (\chi_M)_{\text{calc}}]^2 / \sum[(\chi_M)_{\text{obs}}]^2$, where the J value is in agreement with the value of θ deduced above. It is obviously due to a long-range superexchange pathway between adjacent magnetic centers [32].

4. Conclusions

This work demonstrates that flexible exo-bidentate ligands can be employed in transitional metal M(II) ions (M = Co, Cu)/aromatic chelate ligand/linear ligand systems to generate both 1D helical and 3D pillared helical layer polymers. In contrast to previously reported coordination polymers based on 4,4'-oxy(bisbenzoate) ligand, when employing the chelate ligand 2,2'-dipyridylamine, we obtained three isomorphous coordination polymers with a 1D helical chain through hydrothermal method, namely [Co(oba)(dpa)]_n (**1**), [Cu(oba)(dpa)]_n (**2**) and [Zn(oba)(dpa)]_n [33]. Herein, the presence of chelate ligands in transition metal dicarboxylate systems usually results in the formation of low-dimensional coordination polymers, especially 1D chains, and the employment of a flexible oba ligand may generate helical chains. While the rigid ligand 4,4'-bipyridine is used instead of chelate ligand, the bpy molecule, a linear ancillary ligand, acting as molecular pillar, a novel pillared helical layer coordination polymer ([Cu(oba)(bpy)_{1/2}]_n (**3**)) is produced. The structure of **3** consists of the 2D helical layers, which are connected by bpy pillars to generate a novel 3D framework with an unprecedented topology of (3¹⁵.4²⁰.5⁸.6²), in which two distinct helical chains coexist running along the different crystallographic axis in the 3D network. In addition, the magnetic behavior of complexes **1–3** were investigated and exhibited antiferromagnetic interactions.

Acknowledgments

This work was supported by the National Natural Science Foundation of China (No. 20773104), the Program for New Century Excellent Talents in University (NCET-06-0891), the Nature Scientific Research Foundation of Shaanxi Provincial Education Office of China (No. 06JK155) and the Natural Science Foundation of Shaanxi Provinces of China (No. 2006B08).

Appendix A. Supplementary data

Additional crystallographic data sets for the structures are available through the Cambridge Structural Data Base, as supplementary publication reference number CCDC-661779 for complex **(1)**; CCDC-661778 for complex **(2)** and CCDC-661780 for complex **(3)**. Copies of this information may be obtained from the Director, CCDC, 12 Union Road, Cambridge, CB21EZ, UK (fax: +44 1223 336033; email: deposit@ccdc.cam.ac.uk or <http://www.ccdc.cam.ac.uk>). Supporting information associated with this article can be found, in the online version. The structure of **2**, the sine- and cosine-type curves of the 2D layer in complex **3** viewed along the *c*-axis, the right-handed helical chain is built from bpy bridges between the Cu centers in complex **3** running along the *c*-axis, and TG curve of **1** and **3**.

Supplementary data associated with this article can be found, in the online version, at [doi:10.1016/j.jmolstruc.2007.12.032](https://doi.org/10.1016/j.jmolstruc.2007.12.032).

References

- [1] (a) O.M. Yaghi, M. O'Keefe, N.W. Ockwig, H.K. Chae, M. Eddaoudi, J. Kim, *Nature* 423 (2003) 705;
(b) R. Kitaura, K. Fujimoto, S. Noro, M. Kondo, S. Kitagawa, *Angew. Chem. Int. Ed.* 41 (2002) 133;
(c) S. Kitagawa, R. Kitaura, S.I. Noro, *Angew. Chem. Int. Ed.* 43 (2004) 2334;
(d) X.L. Wang, C. Qin, E.B. Wang, Y.G. Li, Z.M. Su, L. Xu, L. Carlucci, *Angew. Chem. Int. Ed.* 44 (2005) 5824;
(e) C.N.R. Rao, S. Natarajan, A. Choudhury, S. Neeraaj, A.A. Ayi, *Acc. Chem. Res.* 34 (2001) 80;
(f) B. Moulton, M.J. Zaworotko, *Chem. Rev.* 101 (2001) 1629;
(g) X.L. Wang, C. Qin, E.B. Wang, Z.M. Su, *Chem. Eur. J.* 12 (2006) 2680;
(h) S.N. Wang, H. Xing, Y.Z. Li, J.F. Bai, M. Scheer, Y. Pan, X.Z. You, *Chem. Commun.* (2007) 2293.
- [2] (a) G.J. Halder, C.J. Kepert, B. Moubaraki, K.S. Murry, J.D. Cashion, *Science* 298 (2002) 1762;
(b) T.J. Prior, D. Bradshaw, S.J. Teat, M.J. Rosseinsky, *Chem. Commun.* (2003) 500;
(c) A. Galet, M.C. Munoz, J.A. Real, *J. Am. Chem. Soc.* 125 (2003) 14224;
(d) B.Q. Ma, H.L. Sun, S. Gao, *Chem. Commun.* (2003) 2164;
(e) L. Pan, H. Liu, X. Lei, X. Huang, D.H. Olson, N.J. Turro, J. Li, *Angew. Chem. Int. Ed.* 42 (2003) 542;
(f) X.H. Bu, M.L. Tong, H.C. Chang, S. Kitagawa, S.R. Batten, *Angew. Chem. Int. Ed.* 43 (2004) 192.
- [3] (a) D.L. Reger, T.D. Wright, R.F. Semeniuc, T.C. Grattan, M.D. Smith, *Inorg. Chem.* 40 (2001) 6212;
(b) M.B. Zaman, M.D. Smith, H.C. zur Loye, *Chem. Commun.* (2001) 2256;
(c) R. Kitaura, K. Seki, G. Akiyama, S. Kitagawa, *Angew. Chem. Int. Ed.* 42 (2003) 428.
- [4] (a) D.F. Sun, R. Cao, Y.Q. Sun, W.H. Bi, D.Q. Yuan, Q. Shi, X. Li, *Chem. Commun.* (2003) 1528;
(b) S.A. Bourne, J.J. Lu, A. Mondal, B. Moulton, M.J. Zaworotko, *Angew. Chem. Int. Ed.* 40 (2001) 2111;
(c) X.M. Zhang, X.M. Chen, *Eur. J. Inorg. Chem.* (2003) 413;
(d) S.T. Wang, Y. Hou, E.B. Wang, Y.G. Li, L. Xu, J. Peng, S.X. Liu, C.W. Hu, *New J. Chem.* (2003) 1144.
- [5] (a) N.W. Ockwig, O. Delgado-Friederichs, M. O'Keefe, O.M. Yaghi, *Acc. Chem. Res.* 38 (2005) 176;
(b) R. Matsuda, R. Kitaura, S. Kitagawa, Y. Kubota, T.C. Kobayashi, S. Horike, M. Takata, *J. Am. Chem. Soc.* 126 (2004) 14063;
(c) C.N.R. Rao, S. Natarajan, R. Vaidyanathan, *Angew. Chem. Int. Ed.* 116 (2004) 1466.
- [6] S. Kitagawa, R. Kitaura, *Comments Inorg. Chem.* 23 (2002) 101.
- [7] (a) K.T. Holman, A.M. Pivovarov, J.V. Swift, M.D. Ward, *Acc. Chem. Res.* 34 (2001) 107;
(b) M.J. Zaworotko, *Chem. Commun.* (2001) 1.
- [8] G.K.H. Shimizu, G.D. Enright, C.I. Ratcliffe, J.A. Ripmeester, *Chem. Commun.* (1999) 461.
- [9] (a) A. Clearfield, *Prog. Inorg. Chem.* 47 (1998) 371;
(b) D. Medoukali, P.H. Mutin, A. Vioux, *J. Mater. Chem.* 9 (1999) 2553.
- [10] (a) Y.D. Posner, S. Dahal, I. Goldberg, *Angew. Chem. Int. Ed.* 39 (2000) 1288;
(b) H.L. Ngo, W. Lin, *J. Am. Chem. Soc.* 124 (2002) 4298;
(c) J.L. Song, H.H. Zhao, J.G. Mao, K.R. Dunbar, *Chem. Mater.* 16 (2004) 1884;
(d) D.R. Xiao, E.B. Wang, H.Y. An, Y.G. Li, Z.M. Su, C.Y. Sun, *Chem. Eur. J.* 12 (2006) 6528.
- [11] (a) B. Moulton, M.J. Zaworotko, *Chem. Rev.* 101 (2001) 1629;
(b) M. Albrecht, *Chem. Rev.* 101 (2001) 3457;
(c) T. Nakano, Y. Okamoto, *Chem. Rev.* 101 (2001) 4013;
(d) Z. Shi, S.H. Feng, S. Gao, L. Zhang, G. Yang, J. Hua, *Angew. Chem. Int. Ed.* 39 (2000) 2325;
(e) G. Tian, G.S. Zhu, X.Y. Yang, Q.R. Fang, M. Xue, J.Y. Sun, Y. Wei, S.L. Qiu, *Chem. Commun.* (2005) 1396.
- [12] (a) T.E. Gier, X. Bu, P. Feng, G.D. Stucky, *Nature* 395 (1998) 154;
(b) D.R. Xiao, Y. Xu, Y. Hou, E.B. Wang, S.T. Wang, Y.G. Li, L. Xu, C.W. Hu, *Eur. J. Inorg. Chem.* (2004) 1385;
(c) X.L. Wang, C. Qin, E.B. Wang, Y.G. Li, C.W. Hu, L. Xu, *Chem. Commun.* (2004) 378.
- [13] (a) Y. Cui, S.J. Lee, W. Lin, *J. Am. Chem. Soc.* 125 (2003) 6014;
(b) J.P. Zhang, Y.Y. Lin, X.C. Huang, X.M. Chen, *Chem. Commun.* (2005) 1258;
(c) X.L. Wang, C. Qin, E.B. Wang, L. Xu, Z.M. Su, C.W. Hu, *Angew. Chem. Int. Ed.* 43 (2004) 5036;
(d) C.D. Wu, C.Z. Lu, X. Lin, D.M. Wu, S.F. Lu, H.H. Zhuang, J.S. Huang, *Chem. Commun.* (2003) 1284;
(e) O. Mamula, A.V. Zelewsky, T. Bark, G. Bernardinelli, *Angew. Chem. Int. Ed.* 38 (1999) 2945.
- [14] (a) M. Kondo, M. Miyazawa, Y. Irie, R. Shinagawa, T. Horiba, A. Nakamura, T. Naito, K. Maeda, S. Utsuno, F. Uchida, *Chem. Commun.* (2002) 2156;
(b) D.F. Sun, R. Cao, Y.Q. Sun, W.H. Bi, X. Li, M.C. Hong, Y.J. Zhao, *Eur. J. Inorg. Chem.* (2003) 38.
- [15] (a) L. Han, M.C. Hong, R.H. Wang, J.H. Luo, Z.Z. Lin, D.Q. Yuan, *Chem. Commun.* (2003) 2580;
(b) J. Liang, Y. Wang, J.H. Yu, Y. Li, R.R. Xu, *Chem. Commun.* (2003) 882.
- [16] (a) S. Noro, S. Kitagawa, M. Kondo, K. Seki, *Angew. Chem. Int. Ed.* 39 (2000) 2081;
(b) M.L. Tong, H.J. Chen, X.M. Chen, *Inorg. Chem.* 39 (2000) 2235.
- [17] (a) L. Pan, H.M. Liu, S.P. Kelly, X.Y. Huang, D.H. Olson, J. Li, *Chem. Commun.* (2003) 854;
(b) C.S.C. Fernandez, L.M. Thomson, J.R.G. Mascaros, O.Y. Xiang, K.R. Dunbar, *Inorg. Chem.* 41 (2002) 1523;
(c) S.A. Bourne, J.J. Lu, B. Moulton, M.J. Zaworotko, *Chem. Commun.* (2001) 861.
- [18] (a) F.A. Cotton, C. Lin, C.A. Murillo, *Inorg. Chem.* 40 (2001) 478;
(b) G.F. Liu, B.H. Ye, Y.H. Ling, X.M. Chen, *Chem. Commun.* (2002) 1442;
(c) X.J. Li, R. Cao, D.F. Sun, W.H. Bi, Y.Q. Wang, X. Li, M.C. Hong, *Cryst. Growth Des.* 4 (2004) 775.
- [19] (a) F.A.A. Paz, Y.Z. Khimyak, A.D. Bond, J. Rocha, J. Klinowski, *Eur. J. Inorg. Chem.* (2002) 2823;
(b) J. Tao, M.L. Tong, X.M. Chen, *J. Chem. Soc. Dalton Trans.* (2000) 3669;

- (c) P.M. David, M.S. Ronald, L.L. Robert, *Inorg. Chem.* 46 (2007) 7917.
- [20] (a) Z. Shi, S.H. Feng, Y. Sun, J. Hua, *Inorg. Chem.* 40 (2001) 5312;
(b) P. Lightfoot, A. Snedden, *J. Chem. Soc. Dalton Trans.* (1999) 3549.
- [21] (a) X.H. Bu, W. Chen, S.L. Lu, R.H. Zhang, D.Z. Liao, W.M. Bu, M. Shionoya, F. Brisse, J. Ribas, *Angew. Chem. Int. Ed.* 40 (2001) 3201;
(b) D.M.L. Goodgame, D.A. Grachvogel, I. Hussain, A.J.P. White, D.J. Williams, *Inorg. Chem.* 38 (1999) 2057.
- [22] (a) Z.B. Han, X.N. Cheng, X.M. Chen, *Cryst. Growth Des.* 5 (2005) 695;
(b) Y.Z. Zheng, G.F. Liu, B.H. Ye, X.M. Chen, *Z. Anorg. Allg. Chem.* 630 (2004) 296;
(c) Y.B. Wang, Z.M. Wang, C.H. Yan, L.P. Jin, *J. Mol. Struct.* 692 (2004) 77;
(d) M. Kondo, Y. Irie, Y. Shimizu, M. Miyazawa, H. Kawaguchi, A. Nakamura, T. Naito, K. Maeda, F. Uchida, *Inorg. Chem.* 43 (2004) 6139;
(e) G.F. Liu, Z.P. Qiao, H.Z. Wang, X.M. Chen, G. Yang, *New J. Chem.* 26 (2002) 791;
(f) J. Tao, J.X. Shi, M.L. Tong, X.X. Zhang, X.M. Chen, *Inorg. Chem.* 40 (2001) 6328;
(g) C.Y. Sun, X.J. Zheng, S. Gao, L.C. Li, L.P. Jin, *Eur. J. Inorg. Chem.* (2005) 4150.
- [23] G.M. Sheldrick, SADABS, A Program for Empirical Absorption Correction of Area detector Data, University of Göttingen, Germany, 1997.
- [24] G.M. Sheldrick, SHELXS 97, Program for Crystal Structure Solution, University of Göttingen, Germany, 1997.
- [25] G.M. Sheldrick, SHELXL 97, Program for Crystal Structure Refinement, University of Göttingen, Germany, 1997.
- [26] X.M. Chen, G.F. Liu, *Chem. Eur. J.* 8 (2002) 4811.
- [27] X.J. Luan, Y.Y. Wang, L.J. Zhou, X.H. Cai, C.H. Zhou, Q.Z. Shi, *J. Mol. Struct.* 750 (2005) 58.
- [28] C.Y. Sun, L.P. Jin, *J. Mol. Struct.* 782 (2006) 171.
- [29] A.L. Spek, *PLATON*, A Multipurpose Crystallographic Tool, Utrecht, The Netherlands, 2001.
- [30] L.M. Zheng, X.Q. Wang, Y.S. Wang, A.J. Jacobson, *J. Mater. Chem.* 11 (2001) 1100.
- [31] O. Kahn, *Molecular Magnetism*, VCH, New York, 1993.
- [32] (a) P.S. Mukherjee, D. Ghoshal, E. Zangrando, T. Mallah, N.R. Chaudhuri, *Eur. J. Inorg. Chem.* (2004) 4675;
(b) S. Dalai, P.S. Mukherjee, G. Rogez, T. Mallah, M.G.B. Drew, N.R. Chaudhuri, *Eur. J. Inorg. Chem.* (2002) 3292.
- [33] L. Tang, D.S. Li, F. Fu, J.J. Wang, H.M. Hu, Y.Y. Wang, *Chin. J. Chem.* 25 (2007) 1641.